Scientific and Educational Reports of the Faculty
of Science and Technology, Kochi University
Vol. 9 (2026), No. 1

Preliminary X-ray diffraction analyses of the arginine kinase transition-state analogue complex

Chihaya Baba[1], Daichi Yano[2], Yumeto Otsuka[1], Kouji Uda[1], Tomohiko Suzuki[1], Shigeru Sugiyama[1*]

[1]Faculty of Science and Technology, Kochi University, Kochi 780-8520, Japan

[2]Department of Applied Chemistry and Biotechnology, National Institute of Technology, Wakayama College, Wakayama 644-0023, Japan

[*]Correspondence e-mail: ssugiyama@kochi-u.ac.jp

KEYWORDS. arginine kinase, protein crystallization, X-ray crystallography

ABSTRACT: Arginine kinase (AK) from the ciliate *Paramecium tetraurelia* comprises four isozymes, among which *Pt*AK3 uniquely exhibits substrate inhibition, despite sharing high sequence identity with the other family members. To gain structural insight into this unusual catalytic property, we investigated the transition-state analogue (TSA) complex of *Pt*AK3. Crystallization trials of *Pt*AK3–TSA complex yielded three distinct crystal forms. X-ray diffraction data collected at 1.75 Å, 2.30 Å, and 1.60 Å resolution for the Form I, II, and III crystals, respectively, revealed that each form adopts a different space group and unit-cell parameters. Matthews coefficient analysis indicated the presence of one, two, and three *Pt*AK3 molecules per asymmetric unit in the Form I, II, and III crystals, consistent with the monomeric, dimeric, and trimeric noncrystallographic symmetry detected by self-rotation function analysis. These findings suggest that the *Pt*AK3–TSA complex can adopt multiple oligomeric states. Such structural variability may be linked to the substrate-inhibition behavior characteristic of *Pt*AK3. Ongoing structural analysis of each crystal form is expected to clarify how oligomeric assembly and conformational differences contribute to the unique catalytic mechanism of *Pt*AK3.

1. Introduction

Phosphagen kinase (PK) is an enzyme that catalyzes the reversible transfer of the γ-phosphate group from adenosine triphosphate (ATP) to a guanidine substrate, producing adenosine diphosphate (ADP) and a phosphorylated guanidine compound known as a phosphagen (Morrison & James, 1965). These enzymes play a crucial role in maintaining cellular ATP levels, particularly in cells with high energy demands (Ellington, 2001; Ellington & Suzuki, 2006). Arginine kinase (AK), a member of the phosphagen kinase family, has been identified in bacteria (Andrews *et al*., 2008; Suzuki *et al*., 2013) and in protozoan ciliates (Uda *et al*., 2006; Magida & Fraga, 2007), including unicellular organisms.

It is known that arginine kinase (*Pt*AK) from the ciliate *Paramecium tetraurelia* occurs as four subtypes (*Pt*AK1–*Pt*AK4). We previously reported that one of them, *Pt*AK3, exhibits substrate inhibition within the AK family (Yano *et al.*, 2017). Furthermore, we demonstrated that *Pt*AK3 displays a unique type of substrate inhibition in which the enzymatic reaction proceeds to a limited extent even at concentrations that cause inhibition (Yano & Suzuki, 2018). However, comparison of the amino acid sequence of *Pt*AK3 with those of the other three subtypes, which share high sequence identities (70–91%) and do not exhibit substrate inhibition, revealed no notable differences in residues presumed to be involved in catalysis or substrate binding. Therefore, despite the high sequence homology, the fact that only *Pt*AK3 exhibits substrate inhibition is likely attributable to subtle amino acid substitutions that lead to structural variations. Identifying the key residues responsible for this inhibitory behavior may provide insights into the mechanism of substrate inhibition in *Pt*AK3.

We previously reported that diffraction data for ligand-free *Pt*AK3 crystals were collected at 2.60 Å resolution (Otsuka, 2019). In the present study, we further conducted preliminary crystallographic studies on stable enzyme–substrate complexes that mimic the transition state of the enzymatic reaction by obtaining crystals of *Pt*AK3 complexed with a transition-state analog (TSA).

2. Materials and Methods

2.1. Sample preparation and crystallization

Recombinant *Pt*AK3 was expressed and purified as previously described (Yano *et al.*, 2017). The purity of the protein was confirmed by sodium dodecyl sulfate–polyacrylamide gel electrophoresis (SDS–PAGE). For crystallization, the purified *Pt*AK3 solution was concentrated to 5-10 mg/mL using an Amicon Ultra-4 centrifugal concentrator (Merck, USA) and stored at 193 K. Crystallization trials were carried out by the sitting-drop vapor-diffusion method in 96-well plates, employing several commercial screening kits. In each trial, 1.0 µL of the *Pt*AK3–TSA mixture containing 5–10 mg/mL *Pt*AK3, 10 mM Tris-HCl (pH 8.0), and TSA components (8.8 mM Arg, 3.5 mM ADP, 4.4 mM $MgCl_2$, and 16.5 mM $NaNO_3$), was mixed with an equal volume of reservoir solution and equilibrated against 200 µL of the same reservoir solution. All crystallization experiments were carried out at 285 K.

2.2. Data collection

After adding the cryoprotectant, the crystals were picked up at an appropriate cryoloop size and rapidly flash-cooled in

Received: November 17, 2025
Reviewed by anonymous referee, and accepted: January 24, 2026
Published: February 17, 2026

a stream of nitrogen gas at 100 K. X-ray diffraction data were collected using the beamline of the SPring-8 synchrotron-radiation source (Hyogo, Japan). The diffraction intensity data were indexed and integrated using the *XDS* package (Kabsch, 2010) and scaled and merged using the Aimless program of the *CCP4* program package (Evans & Murshudov, 2013).

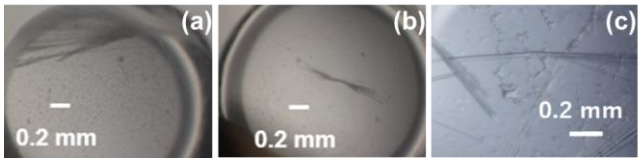

Figure 1.
Crystals of the *Pt*AK3–TSA complex. (a) Form I; (b) Form II; (c) Form III.

3. Results and Discussion

Crystals obtained from the *Pt*AK3–TSA mixed solution appeared as needle-like crystals when PEG4000 or ammonium sulfate was used as a precipitant. These crystals occurred in three distinct crystal forms, designated as the Forms I, II, and III. Crystals suitable for X-ray diffraction were obtained under the following conditions: the Form I crystals were grown from a reservoir solution containing 30% (w/v) PEG4000 and 0.1 M Tris–HCl (pH 8.5); the Form II crystals were obtained from a reservoir solution containing ammonium sulfate and 0.1 M HEPES–NaOH (pH 7.5); and the Form III crystals were obtained from a reservoir solution containing 30% (w/v) PEG4000 and 0.1 M HEPES–NaOH (pH 7.5). These results suggest that the *Pt*AK3–TSA complex may adopt multiple conformations or oligomeric states, although the possibility remains that these differences arise from variations in crystallization conditions.

Table 1.
Crystal parameters and data-collection statistics for *Pt*AK3.

	Form I	Form II	Form III
Space group	$P3_121$	$P2_1$	$C2$
Unit-cell parameters			
a (Å)	126.9	50.1	220.6
b (Å)	126.9	151.1	124.9
c (Å)	49.5	57.7	49.3
α, β, γ (°)	90, 90, 120	90, 96, 90	90, 90.2, 90
Resolution range (Å)	45.18–1.75	47.36–2.30	49.38–1.60
(High-resolution shell)	(1.78–1.75)	(2.38–2.30)	(1.63–1.60)
No. of unique reflections	46,386	37,384	170,639
Completeness (%)	100 (100)	98.8 (97.2)	97.2 (96.1)
Multiplicity	30.8 (30.3)	10.0 (9.9)	7.9 (7.3)
Mean $I/\sigma(I)$	18.2 (2.1)	6.8 (2.1)	3.2 (1.1)
R_{pim} (%)	7.4 (78.2)	30.7 (200.7)	20.9 (116.8)
CC(1/2)	0.99 (0.79)	0.94 (0.76)	0.87 (0.57)

Values in parentheses are for the outer shell.

Diffraction studies were performed at cryogenic temperature. The crystals were soaked rapidly in the 25% (v/v) glycerol as a cryoprotectant and then rapidly flash-cooled. The Form I, II, and III crystals diffracted to 1.75, 2.30, and 1.60 Å resolution using synchrotron radiation, respectively. Analysis of the symmetry and systematic absences in the X-ray diffraction data revealed that the Form I, II, and III crystals represent distinct crystallographic forms with different space groups and unit-cell parameters. Specifically, the three crystal forms exhibited distinct space groups and unit-cell parameters: Form I, trigonal $P3_121$ (a = b = 126.9 Å, c = 49.5 Å); Form II, monoclinic $P2_1$ (a = 50.1 Å, b = 151.1 Å, c = 57.7 Å); and Form III, monoclinic $C2$ (a = 220.6 Å, b = 124.9 Å, c = 49.3 Å). The crystal parameters and data-collection statistics are summarized in Table 1.

Using the diffraction data obtained from the Form I, II, and III crystals, Matthews coefficient analysis (Matthews, 1968) was performed. The results indicated that the Form I crystal contains one molecule per asymmetric unit with a solvent content of 52.3% (V_M = 2.58 Å³/Da). The Form II crystal contains two molecules per asymmetric unit with a solvent content of 49.6% (V_M = 2.44 Å³/Da), and the Form III crystal contains three molecules per asymmetric unit with a solvent content of 51.7% (V_M = 2.54 Å³/Da).

Table 2.
Self-rotation function analysis.

Form I	θ (°)	φ (°)	χ (°)	P/P_0
1	90.00	-164.38	180.00	0.13
2	136.99	90.00	180.00	0.12
3	90.00	-154.16	180.00	0.11
Form II	θ (°)	φ (°)	χ (°)	P/P_0
1	90.00	0.00	180.00	0.64
2	82.43	180.00	180.00	0.20
3	13.10	-50.43	180.00	0.14
Form III	θ (°)	φ (°)	χ (°)	P/P_0
1	180.00	0.00	120.01	0.76
2	77.24	180.00	180.00	0.16
3	90.54	116.96	180.00	0.15

P/P_0 represents the relative height of the self-rotation function peak compared with the origin peak calculated by *MOLREP*.

The self-rotation function was calculated using the program *MOLREP* (Vagin & Teplyakov, 1997). No significant peaks were detected for the Form I crystal. In the Form II crystal, a prominent peak (polar angles θ = 90°, φ = 0°, χ = 180°) 3.2 times higher than the second peak was observed in the χ = 180° section, indicating the presence of noncrystallographic twofold symmetry. The position of this peak suggested that the noncrystallographic twofold axis is nearly perpendicular to the crystallographic b-axis. In the Form III crystal, a strong peak (θ = 180°, φ = 0°, χ = 120°) 4.7 times higher than the second peak was observed in the χ = 120° section, indicating the presence of noncrystallographic threefold symmetry.

These results are consistent with the Matthews coefficient analysis, which indicated that the Form I, II, and III crystals contain one, two, and three *Pt*AK3 molecules per asymmetric unit, respectively. Furthermore, the self-rotation function confirmed that the Forms I, II, and III correspond to

monomeric, dimeric, and trimeric assemblies, respectively. This finding suggests that the *Pt*AK3–TSA complex can adopt multiple oligomeric states, which may be related to the enzymatic reaction and substrate-inhibition mechanism of *Pt*AK3. Structural analysis of all three crystal forms of the *Pt*AK3–TSA complex is currently in progress.

Acknowledgements

The synchrotron-radiation experiments were performed at SPring-8 with the approval of the Japan Synchrotron Radiation Research Institute (JASRI; Proposals 2022B6717, 2022A/B2731, 2023A/B6815, 2023A/B2729, 2024A6915, and 2024A/B2717).

References

Andrews, L.D., Graham, J., Snider, M.J., & Fraga, D., *Comp. Biochem. Physiol. B Biochem. Mol. Biol*., **150**, 312–319 (2008).

Ellington, W.R., *Ann. Rev. Physiol.*, **63**, 289–325 (2001).

Ellington, W.R., & Suzuki, T., In: Vial C (ed) Molecular anatomy and physiology of proteins: creatine kinase. Nova Science, New York, pp 1–27 (2006).

Evans, P.R. & Murshudov, G.N., *Acta Crystallogr. D*, **69**, 1204–1214 (2013).

Kabsch, W., *Acta Crystallogr. D*, **66**, 133–144 (2010).

Magida, L. & Fraga, D., *FASEB J*., **21**, A299 (2007).

Matthews, B.W., *J. Mol. Biol.*, **33,** 491-497 (1968).

Morrison, J.F., & James, E., *Biochem. J.*, **97**, 37–52 (1965).

Otsuka, Y., Yano, D., Tanaka, J., Uda, K., Suzuki, T., Sugiyama, S., *Sci. Educ. Rep. Fac. Sci. Technol. Kochi Univ.*, **2**, 16-26 (2019).

Suzuki, T., Soga, S., Inoue, M., & Uda, K., *Int. J. Biol. Macromol.*, **57**, 273-277 (2013).

Vagin, A. & Teplyakov, A., *Acta Crystallogr. D*, **66**, 22-25 (2010).

Uda, K., Fujimoto, N., Akiyama, Y., Mizuta, K., Tanaka, K., Ellington, W.R., & Suzuki, T., *Comp. Biochem. Physiol. Part D Genomics Proteomics*, **1**, 209-218 (2006).

Yano, D., Suzuki, T., Hirokawa, S., Fuke, K., & Suzuki, T., *Int. J. Biol. Macromol.*, **101**, 653–659 (2017).

Yano, D., & Suzuki, T., *Protein J.*, **37**, 581-588 (2018).